

A High Dynamic Range CMOS Image Sensor With Dual-Exposure Charge Subtraction Scheme

Xinyuan Qian, Hang Yu, Shoushun Chen, *Member, IEEE*, and Kay Soon Low, *Senior Member, IEEE*

Abstract—In this paper, we present a CMOS image sensor for star centroid measurement for the application of star trackers. We propose a new capacitive transimpedance amplifier pixel architecture with in-pixel charge subtraction scheme. The pixel is able to achieve high signal-to-noise ratio for dim stars and, at the same time, to avoid saturation for bright stars. A prototype sensor was fabricated using Global Foundry 65-nm mixed-signal CMOS process. Experimental results show that the sensor can achieve 3.8 V/lux·s and 12 dB extension of dynamic range. For the saturated star in conventional method, the centroiding accuracy is improved by over 0.1 pixels after performing charge subtraction.

Index Terms—CMOS image sensor, capacitive transimpedance amplifier (CTIA), high dynamic range (HDR), star tracker.

I. INTRODUCTION

A STAR tracker uses a CMOS image sensor to capture the star field, as illustrated in Fig. 1. Star centroids such as $A(X_{c,A}, Y_{c,A})$ are then calculated to build a star pattern. The pattern is finally delivered to a recognition algorithm to determine the satellite attitude [1]. For satellites operated in orbit, long exposure will cause “tail effect” (e.g. star B) in the captured star image, leading to degradation in centroiding accuracy; short exposure will result in limited signal to noise ratio (SNR). In addition, bright stars can easily saturate the pixels, which can also induce significant centroiding error.

This letter presents a CMOS image sensor for star centroid measurement. We propose a new pixel architecture based on CTIA pixel [2] to provide high sensitivity to detect dim stars accurately. The pixel also features a scheme of in-pixel charge subtraction to extend the dynamic range for bright stars.

II. PIXEL ARCHITECTURE

The pixel schematic is shown in Fig. 2. It consists of a fundamental CTIA pixel, circuits for charge subtraction, a comparator with D flip flop (DFF), and readout circuits. In CTIA pixel, the photodiode is held at a constant voltage

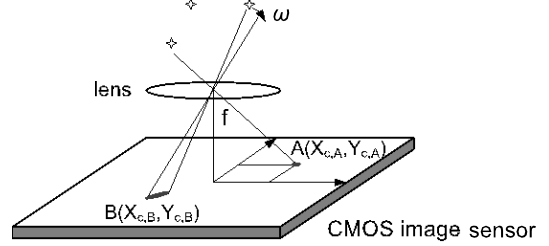


Fig. 1. CMOS image sensor maps the star field onto the focal plane. Star centroids are calculated from the star spots in the captured image.

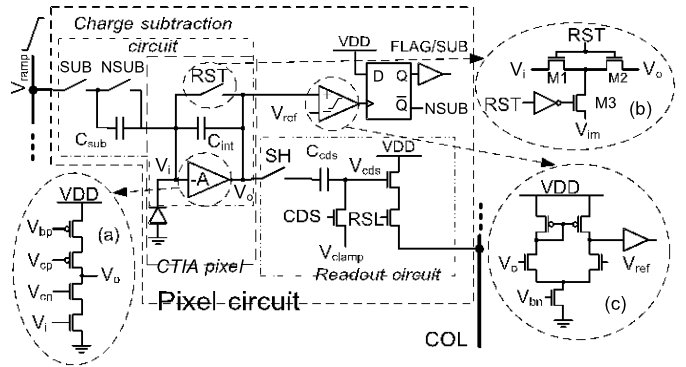


Fig. 2. The schematic of the pixel circuit. (a) The schematic of the OTA. (b) The reset switch. (c) The comparator are shown respectively.

and photocurrent is integrated on C_{int} . The output follows:

$$V_o \approx \frac{1}{C_{int}} \int I_{ph} dt \quad (1)$$

The schematic of the OTA (Fig. 2(a)) is a single-ended cascode common-source amplifier. The reset switch (Fig. 2(b)) is a “T-type” switch to prevent subthreshold leakage from V_o to V_i . The external bias V_{im} is set close to V_i . The comparator (Fig. 2(c)) is an open-looped five-transistor OTA with a digital buffer. The readout circuit features a clamp circuit for in-pixel Correlated Double Sampling (CDS). The source follower drives the column bus when the row is selected.

Fig. 3 shows the timing diagram of the pixel. The pixel has two equal-length exposures (T_{int}). In first exposure, pixel voltage is compared with a reference threshold V_{ref} to determine whether the pixel requires charge subtraction. If the photocurrent is small, the comparator does not toggle, as the case in Fig. 3(a), DFF will not be triggered to reconfigure the pixel circuit. Hence, both exposures have the same response. The photocurrent can be simply expressed as:

$$I_{ph} = \frac{C_{int} \cdot V_o}{T_{int}} \quad (2)$$

Once V_o reaches V_{ref} in the first exposure, as the case in Fig. 3(b), DFF will then reconfigure the switches associated

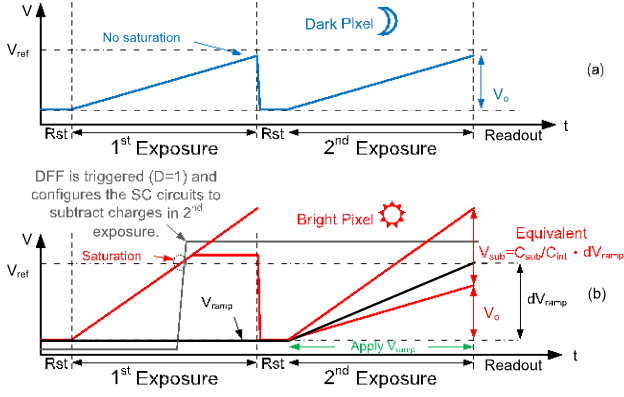


Fig. 3. Pixel operation timing diagram in (a) dark and (b) bright conditions.

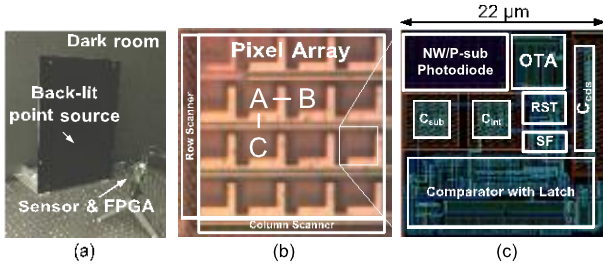


Fig. 4. (a) Test setup. (b) Chip microphotograph. (c) Pixel layout.

with C_{sub} . It connects C_{sub} to a column bus driven by a ramp signal (V_{ramp}). V_{ramp} rises as the second exposure starts, which continuously subtracts the charges from the integration results. The amount of subtracted charges is designed to be the well capacity of the pixel. The photocurrent can then be expressed as:

$$I_{ph} = \frac{C_{int} \cdot V_o + C_{sub} \cdot dV_{ramp}}{T^{int}} \quad (3)$$

Since the DFF stores the information whether the pixel conducts charge subtraction, the pixel outputs both pixel voltage (V_o) and digital signal ($FLAG$) for image reconstruction.

III. PROTOTYPE CHIP AND MEASUREMENT RESULTS

Fig. 4(a) shows the test setup with the prototype chip. The sensor is illuminated by back-lit point sources in a dark room. Fig. 4(b) and (c) show the prototype chip with 4×4 pixels and pixel layout implemented in 3.3 V devices with Global Foundries 65 nm mixed-signal CMOS process, respectively. The pixel is $22 \times 22 \mu\text{m}^2$ and uses a N-well/P-sub photodiode. C_{int} and C_{sub} are designed to be 10 fF. The value of C_{cds} is 28 fF. Fig. 5 shows the measured photocurrent with incident light intensity. The sensitivity is about $3.8 \text{ V/lux} \cdot \text{s}$. With charge subtraction, DR increases about 12 dB. Table. I summarizes the sensor performance and comparison with a commercial star sensor (Cypress STAR-1000).

Three point sources are projected at the centers of pixel A, B, and C to simulate “star” signals, as shown in Fig. 4(b). The lens is slightly defocused to spread the signal in a 3×3 pixel region. The centroids are calculated by center-of-mass algorithm in this region [3]. Centroid distance AB and AC are compared. Fig. 6 shows this distance error at different exposure time. The centroiding accuracy increases

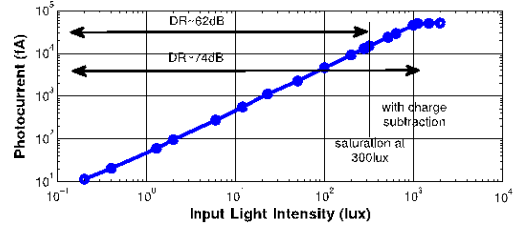


Fig. 5. Measured photocurrent with regard to incident light intensity. The pixel saturates at around 300 lux. With charge subtraction, the dynamic range increases by approximately 12dB and saturates at around 1100 lux.

TABLE I
PERFORMANCE SUMMARY AND COMPARISON

Specification	STAR-1000	This work
Technology	NA	GF 65 nm CMOS
Pixel Size	$15 \times 15 \mu\text{m}^2$	$22 \times 22 \mu\text{m}^2$ (FF = 14%)
Conversion Gain	$11.4 \mu\text{V}/e^-$	$16 \mu\text{V}/e^-$
Signal Swing	1.1 V	1.38 V
Dark Current	$223 \text{ pA}/\text{cm}^2$	$992 \text{ pA}/\text{cm}^2$
Random Noise	35 e-	$980 \mu\text{V}$ (61 e-)
FPN	0.56%	0.73%
SNR	NA	62 dB at full swing
Dynamic Range	72 dB	62 dB (74 dB with charge subtraction)

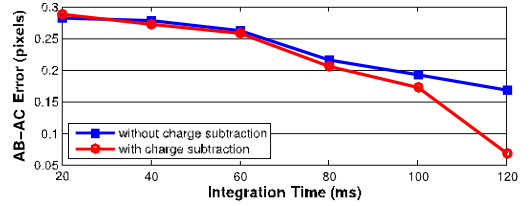


Fig. 6. Measured $AB-AC$ distance error at different integration times. “star” pixels does not saturate when integration time is small, so charge subtraction does not improve the error obviously. However, saturation occurs in “stars” after about 80 ms. With charge subtraction, centroiding accuracy improves much better compared with the saturated one.

with exposure time due to increased signal magnitude and its SNR. After pixel saturation, no further obvious improvement on centroiding accuracy is observed. With charge subtraction, the pixel can still accurately quantize the photocurrent and the centroiding accuracy continues improving.

IV. CONCLUSION

The design of a centroid measurement CMOS image sensor for star trackers is described. A new CTIA pixel architecture with in-pixel charge subtraction is proposed for accurate starlight measurement. A proof-of-concept chip has been fabricated in Global Foundry 65 nm CMOS process. Measurement results show that the sensor achieves $3.8 \text{ V/lux} \cdot \text{s}$ sensitivity with a $22 \times 22 \mu\text{m}^2$ pixel and 12 dB increase of dynamic range. After performing charge subtraction, the centroiding accuracy of saturated stars is improved by over 0.1 pixels.

REFERENCES

- [1] M. D. Pham, K.-S. Low, and S. Chen, “An autonomous star recognition algorithm with optimized database,” *IEEE Trans. Aerosp. Electron. Syst.*, vol. 49, no. 3, pp. 1467–1475, Jul. 2013.
- [2] K. Murari, R. Etienne-Cummings, N. V. Thakor, and G. Cauwenberghs, “A CMOS in-pixel CTIA high-sensitivity fluorescence imager,” *IEEE Trans. Biomed. Circuits Syst.*, vol. 5, no. 5, pp. 449–458, Oct. 2011.
- [3] C. C. Liebe, “Accuracy performance of star trackers—A tutorial,” *IEEE Trans. Aerosp. Electron. Syst.*, vol. 38, no. 2, pp. 587–599, Apr. 2002.